Heat transfer in rock masses: Application to the Lascaux Cave (France)

F. Salmon*, D. Lacanette, H. Lharti, C. Sirieix

Université de Bordeaux, CNRS, ENSAM, Bordeaux-INP, INRA, UMR 5295 I2M, 33405 Talence, France

Keywords:
Conduction
Evapotranspiration
Caves
Rock mass

The conservation of prehistorical painted caves is a major issue for the history of mankind. Alterations, which can appear on walls, mainly result from the thermal convection taking place in caves. The convection in caves depends on the difference between the temperatures of the walls which mainly stem from the heat conduction in rock masses. In literature, this problem is currently solved with a uni-dimensional homogeneous model where the outside air temperature is the only source of energy. Here, based on the literature in other fields, we show that the ground surface temperature cannot be considered as equal to the outside temperature. Radiation, convection and water evaporation indeed figure prominently in the process. The mathematical guideline giving the topsoil temperature is detailed. In addition, we propose a mathematical assumption to ensure energy conservation. A simple experimental setup allowing the circumvention of this complex procedure is also suggested. Then, we apply the widely used uni-dimensional homogeneous thermal diffusion model, with the proposed ground surface temperature calculation, to the Lascaux Cave. The comparison between the measurements in the first meter below the ground surface and the calculated temperatures shows a good agreement. Within the cave, the model successfully predicts the temperature measured by a few thermocouples. For others, there are significant discrepancies, which seem to indicate that the homogeneous hypothesis is not precise enough to describe rock masses. The heterogeneity of the Lascaux Cave massif will thus need to be thermally investigated.

1. Introduction

Heat transfer in soil concerns different fields such as underground waste storage, geothermics, ground-coupled heat exchangers, mines, electrical resistivity tomography, caves, etc. Today, this physical process remains difficult to predict due to the intrinsic complexity of soils and rocks. Scientists have thus worked on improving our understanding of heat transfer in soils and rock. Lönnqvist and Hökmark [1] studied heat transfer in the rock mass surrounding a waste container to understand its thermo-mechanical behavior. Driving by the same issue, Sultan et al. [2] investigated the thermo-mechanical properties of specific clay. Salt caverns, which store gas, hydrogen or oil for instance, also require the study of thermal conduction in rock around them [3]. This question is also of great interest in the renewable energy domain. Heat exchangers reduce air temperature thanks to the damping of thermal waves underground. Thermal diffusion is thus widely studied by domain experts [4,5]. More particularly, heat transfer inside boreholes is the main challenge for these researchers.

Tackling heat transfers in ground is also a paramount issue for the conservation of cultural sites such as painted caves. The temperature inside caves is indeed driven by weather conditions and heat transfers in rock. The temperature differences between cave walls can then induce thermal convection [6,7] and indirectly threaten paintings through thermally-dependent processes damaging them. Several studies [8–10] thus tried to assess the heat transfer in rock mass like in a Slovenian cave [11]. Perrier et al. [12] instrumented a Japanese cavity to measure temperature differences between the floor and the ceiling of the cave. All these authors measure temperature variations in the caves compatible with those theoretically expected due to thermal conduction in the rock masses. The temperature in closed shallow caves thus result from the propagation of annual thermal waves from the ground surface. On the contrary, the geothermal heat flux is most of time very low close to the ground surface in comparison with the conductive heat flux. It has been shown that in a karst system, the geothermal heat flux is drained off and does not affect the temperature [13,14]. For instance, Perrier et al. [12] have compared the geothermal heat flux at Yokosuka to the conductive heat flux in an underground vault at Aburatsubo. They have found that the former was 13 times smaller than the latter.

In the field of cave conservation, the heat transfer modeling relies on the hypothesis that energy propagates by thermal diffusion

* Corresponding author.
E-mail address: Fabien.Salmon@u-bordeaux.fr (F. Salmon).

https://doi.org/10.1016/j.ijheatmasstransfer.2023.124029

in homogeneous rock. In the previously mentioned researches in this field, the model consists of solving the heat equation with the outside temperature as the ground surface temperature. However, physicists dealing with the superficial temperature of topsoils (thin upper soil layer supporting microscopic life) [15,16], perform instead an energy balance on the ground surface. It includes radiation, convection, conduction and also phase changes. This matter is particularly well referenced in the agriculture domain. Some researches indeed focus on the topsoil temperature to optimize harvests and always consider the influence of radiation and evapotranspiration (ETP) in the process [17–19].

In this article, we propose a methodology to model the heat transfer in cave rock masses. This approach is applied to the Lascaux Cave (France), one of the most famous painted caves in the world [20]. This cave was discovered in 1940 and represented a major breakthrough in archaeology due to the amount and the quality of paintings. It was open to the public in 1948 and very visited until its closure in 1963 due to major preservation issues. Then, a scientific committee, dedicated to advise about the cave conservation, was created. It relies on approximately 150 sensors which have measured the temperature inside and outside the cave for decades. We compare our model with some of these measurements in the top part of the rock mass and within the cave. We show the great importance of the ground surface temperature in this physical problem both experimentally and theoretically. We then discuss the limits of our modeling, especially for deep parts inside the cave. We finally address the developments necessary to improve temperature predictions.

2. Experimental setup

The study is conducted on the Lascaux Cave, located in Dordogne (France). Fig. 1 presents the 3D geometry of the Lascaux Cave within the surrounding rock mass. The topographic surface is represented in green. The ground elevation slowly increases from South to North and from West to East. The cavity penetrates the rock up to more than 20 m. The thickness of the topsoil is between 5 and 10 cm. Deeper, the rock mass is mainly made of Upper Cretaceous limestone, Santonian in the upper part and Coniacian below 182 m NGF (Nivellement général de la France), but is known to be highly heterogeneous and composed of different kinds of materials [21–23]. Fig. 2 displays the top view of the 3D resistivity model of the Lascaux massif developed by Xu et al. [22]. It is based on measurements achieved with the electrical resistivity tomography method. The high variations of resistivity demonstrate a great heterogeneity of the massif with different kinds of materials depending on the locations and the depths. The Lascaux hill is partially covered by trees such as oaks, pines and chestnuts. Pines are mainly in the West on detrital formations which corresponds to sandy clay (lower resistivity). Chesnuts are mainly in the East on sand (higher resistivity). The central part, where there is the cave, is composed of limestone.

The cave is closed and thermally insulated at the entrance with four successive insulated chambers. This avoids air exchange at the entrance. Sensors measure the temperature inside the cavity and close to the ground surface, 50 cm and 100 cm in depth. The thermocouples are located throughout the cave, so at different depths (Fig. 3). Within the cave, the thermocouples are located 3 cm in the walls. The uncertainty on the depth is one millimeter and the holes have been patched to avoid measuring the air temperature. At the ground surface, we have pierced holes 50 or 100 cm deep. The uncertainty is estimated to smaller than 0.5 cm. We use ALMENO 2890 9-input data loggers with 36 channels. The thermocouples are PT-100 sensors with a sensibility of 10^{-3} °C and present a relative precision between them of 10^{-2} °C.

In addition to these sensors, measurements are continuously achieved outside. Net radiation, relative humidity, wind speed and outside temperature are measured at three locations approximately one meter above the ground: O0, P0 and S0 (Fig. 3). These points correspond to three different configurations: beneath oaks (medium radiation), beneath pines (low radiation) and in direct sunlight (high radiation). In the following, we refer to configurations O, P and S respectively. They will be associated with the measurements achieved at 50 and 100 cm below the ground surface presenting the same initial letter in Fig. 3. The outside thermocouples present shelters in order to avoid them to be affected by radiation.

3. Strategy to model heat transfer in rock masses

The heat transfer in rock mostly corresponds to thermal diffusion. As indicated in the introduction, this process involves thermal convection in shallow caves. Due to the seasonal variations of temperature, the temperature profile against depth is not strictly decreasing as shown in Fig. 4. This can lead, depending on the time of year, to a downward temperature gradient within the cave, which can initiate thermal convection. In the Lascaux Cave, the Rayleigh number can reach 10^8, so turbulent convection can occur [7].

However, as noted in the introduction, the ground surface temperature should result from a complex energy balance involving radiation, convection, conduction and phase changes.

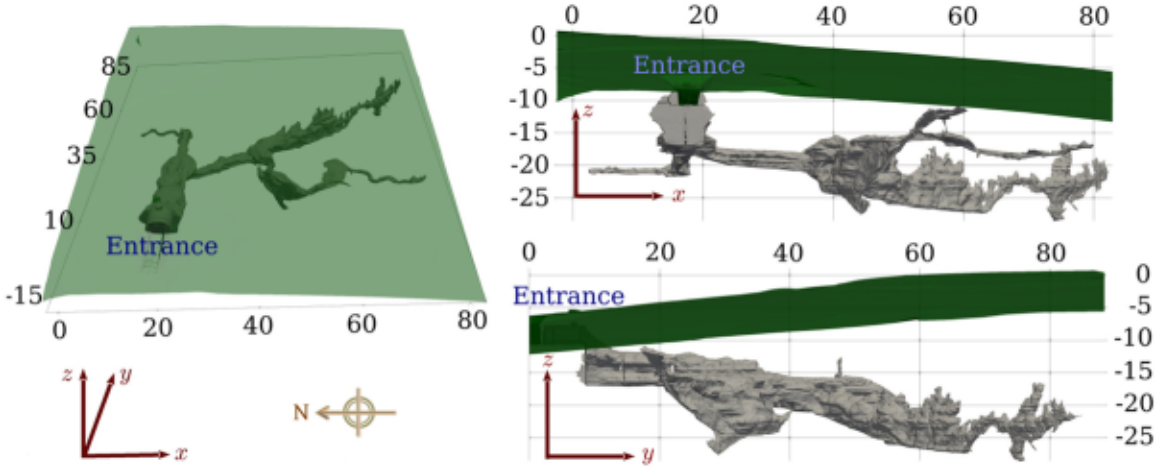

Fig. 1. Lascaux Cave geometry with the topographic surface in green. Both figures on the right correspond to orthogonal projections of the ground surface and the cavity on the xz and yz planes.

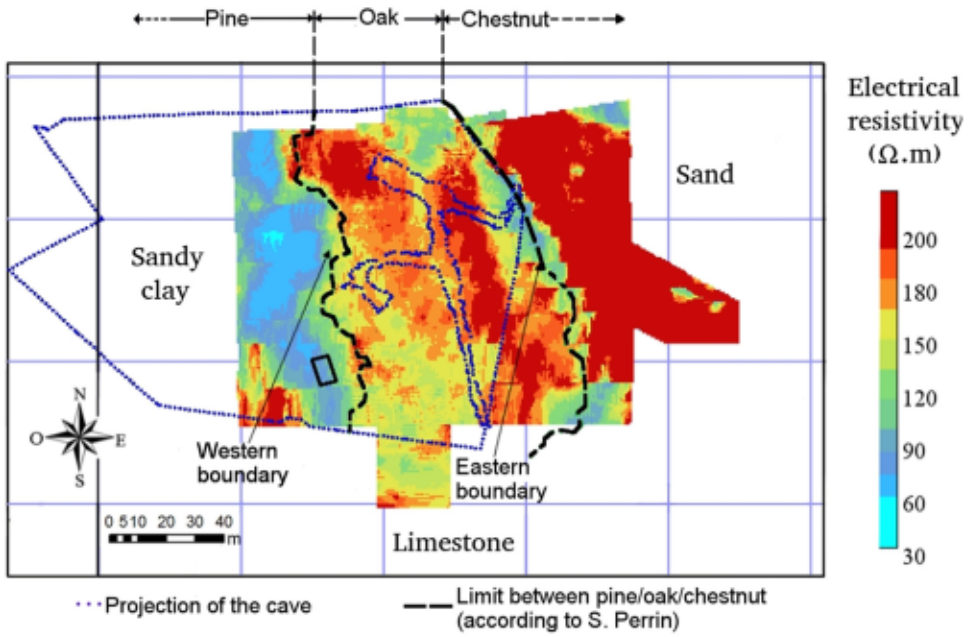

Fig. 2. Superficial electrical resistivity measurements at the Lascaux site [22]. The East formations correspond to sand, the center formations to limestone and the West formations to sandy clay.

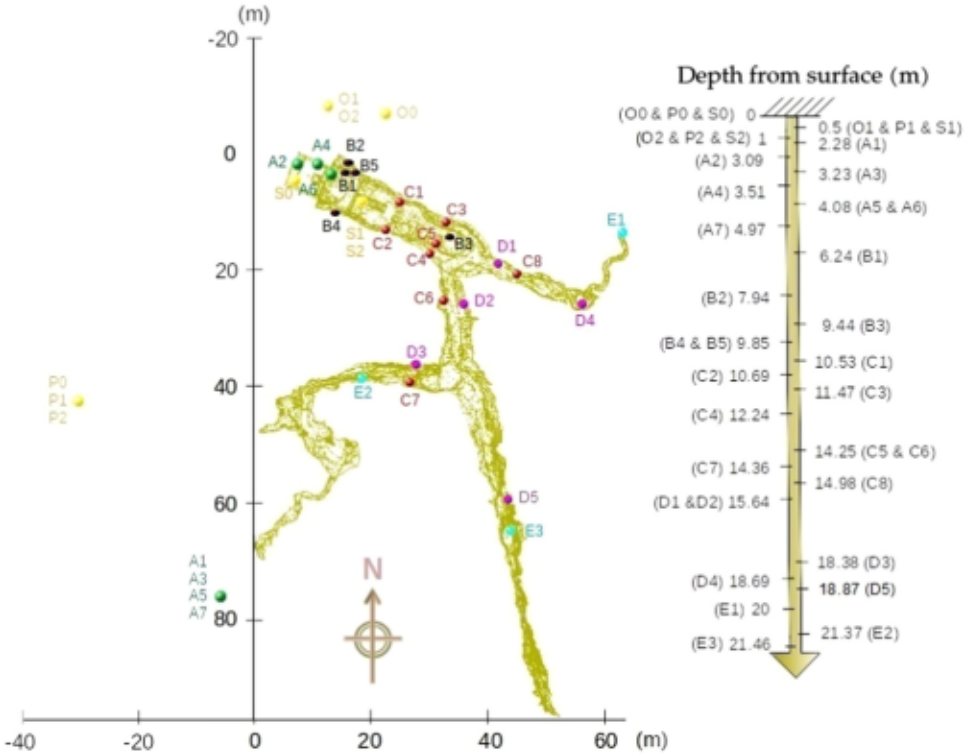

Fig. 3. Cutaway view of the Lascaux Cave with the locations of each thermocouple. The vertical arrow on the right presents the depth of the sensors from the ground surface right above them. O0, P0 and S0 correspond to outside measurements at approximately 1 meter above ground.

3.1. Thermal diffusion in rock masses

Thermal diffusion is governed by the heat equation. In this paper, we consider homogeneous rock thermal properties. This hypothesis is commonly used in such studies [8–12] as explained in the introduction. However, karstic massifs are often very heterogeneous and, as described in Section 2, the Lascaux rock mass is composed of different materials. The homogeneous hypothesis can therefore appear to be a rough assumption. We will discuss the reliability of this hypothesis in Section 5 in light of the results obtained by the following model. We also assume the diffusion to occur in one dimension:

$$\frac{\partial T}{\partial t} = D\frac{\partial^2 T}{\partial z^2} \tag{1}$$

where T is the temperature (°C) and D the thermal diffusivity of the material ($m^2.s^{-1}$).

Fig. 4. Typical temperature profile in a rock mass resulting from conductive heat transfer. The downward temperature gradient stemming from the ceiling temperature which becomes colder than the floor temperature ($T_{ceiling} < T_{floor}$) can lead to the onset of thermal convection.

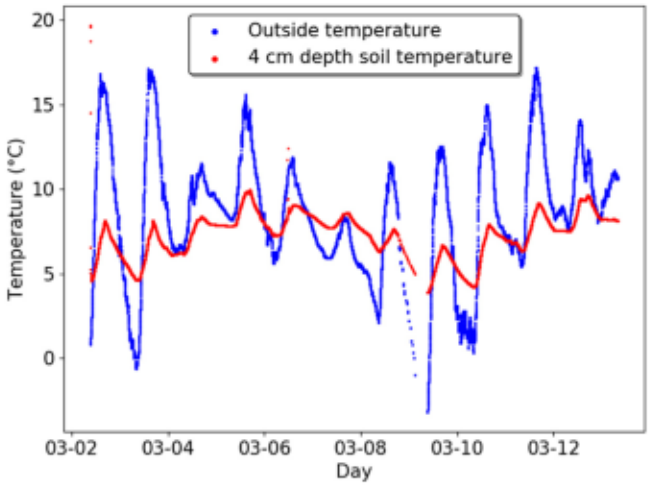

Fig. 5. Measured temperature of air and approximately 4 cm deep in the topsoil over 11 days.

The thermal diffusivity of rock is difficult to measure on site. Using core samples are scarcely possible in a cultural heritage site. Moreover, they do not reflect the *in situ* thermal processes due to existing water circulations and fractures within any superficial rock mass which do not happen in a sample while having a significant impact on thermal properties. This circulation is linked with the porosity of rock masses composed of two contributions. First, the matrix porosity is the intrinsic porosity of the studied material, here limestone presenting a matrix porosity of approximately 5% [24]. Second, the fracture porosity characterizes the additional hollow space due to fractures. This cannot be measured on samples whereas it reaches up to 30% for Lascaux [25]. When these fractures are filled with water or clay, they significantly modify the thermal diffusivity of rock. Sample measurements are therefore meaningless for this kind of study.

In order to assess the averaged thermal diffusivity of rock, we propose to use the analytical solution of Eq. (1) in the case of a sinusoidal outside temperature

$$T(z,t) = T_{mean} + \frac{T_{max} - T_{min}}{2} e^{-\sqrt{\frac{\pi}{\theta D}}z} cos\left(\frac{2\pi}{\theta}t - \sqrt{\frac{\pi}{\theta D}}z\right) \quad (2)$$

where T_{min} and T_{max} are the minimal and maximal temperatures of the thermal wave respectively and T_{mean} is the average temperature over a period θ.

The genuine outside temperature does not strictly follow a sinusoid but is close to it with a period θ of one year and a magnitude $T_{max} - T_{min}$ of approximately 15 °C. In such a case, at depth z, thermal diffusion produces a phase change $\delta\phi$ (months) and a thermal damping γ (dimensionless) equal to

$$\delta\phi = z\sqrt{\frac{\theta}{4\pi D}} \quad (3)$$

$$\gamma = e^{-z\sqrt{\frac{\pi}{\theta D}}} \quad (4)$$

Based on graphical estimations of the phase change and the thermal damping measured by each thermocouple, Eqs. (3) and (4) provide two rock thermal diffusivities which should be equal in a homogeneous medium. It is worth noting that the estimation of thermal diffusivities with phase change is more accurate than with damping since there is no uncertainty on the wave period (one year), whereas the wave magnitude depends on weather and can slightly differ from 15 °C.

In Section 4.1, we will assess the rock thermal diffusivity from all the sensors based on Eqs. (3) and (4). According to the results, one can keep the averaged thermal diffusivity or consider that the thermal properties cannot be supposed homogeneous. In the latter case, a better knowledge of the site geology is needed. In Sections 4.2 and 4.3, the calculated temperatures refer to the resolution of Eq. (1) based on finite differences. The Euler scheme is used to discretized the temporal derivative while the second order spatial derivative is discretized with a second order centered scheme. The explicit resolution relies on a spatial step of 20 cm for cave thermocouples (Section 4.3) and 5 cm for thermocouples close to the ground surface (Section 4.2). The time step respects the mathematical condition for numerical stability $\Delta t < 0.5\frac{\Delta x^2}{D}$. The domain length is 40 m to avoid any boundary influences. A zero Neumann boundary condition is considered at this depth. At the surface, where $z = 0$, a Dirichlet boundary condition is applied. The value of the imposed temperature results from the ground surface temperature computation (Section 3.2). The initial condition in temperature relies on the analytical solution (Eq. (2)) of the heat equation. The parameters in the equation are adjusted to the measurements of the year 2000, which is the starting point of the resolution. Beginning far before the period of interest is enforced by the huge thermal inertia of the rock mass. The initial condition being inevitably different from the actual rock temperature at this time, the difference must be reduced after several wave periods.

3.2. Ground surface temperature computation

We first show that shallow measurements at Lascaux cannot only be explained by the outside air temperature. We then detail the mathematical procedure to estimate the ground surface temperature.

3.2.1. Outside and topsoil temperature

In order to compare the air temperature and the temperature of the topsoil surface, we added a thermocouple approximately 4 cm into the topsoil at the same location as S1 and S2, so in direct sunlight (Fig. 3). Fig. 5 compares the measurements over 11 days in March 2022.

The phase change is approximately 2 h. According to Eq. (3), with a wave period of one day, this means that the topsoil thermal diffusivity is between $10^{-7} m^2.s^{-1}$ and $2 \times 10^{-7} m^2.s^{-1}$. This low value stems from the intrinsic composition of soils, and belongs to the expected range [26]. Such a diffusivity yields a damping of 40%. Fig. 5 clearly shows that the temperature amplitude in depth is far smaller than 60% of the amplitude of the surface temperature.

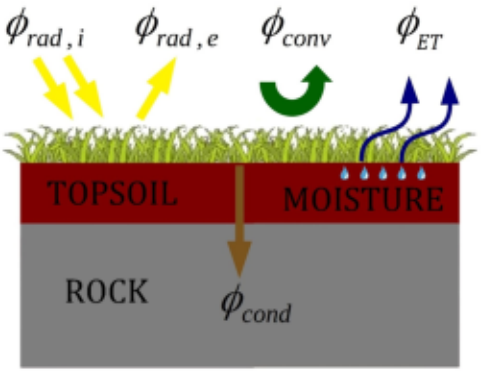

Fig. 6. Energy balance at the ground surface.

In addition, the average temperature over a period does not depend on depth. Considering the air temperature as the ground surface temperature, as it is currently done in cave literature, thus requires the assumption that the daily average air temperature is equal to the daily average temperature a bit deeper in the ground. Note that the depth in soil must be small enough for the phase changes to be negligible since the daily average temperature varies according to time. The 11-days average of both temperatures gives approximately 8.7 °C for the air and 7.3 °C in depth. This means that there is a significant loss of energy near the ground surface.

This study clearly reveals an inconsistency between the measurements and the hypothesis about the surface temperature. We will see in the next section how the ground surface temperature must be calculated.

3.2.2. Energy balance

The temperature at the surface of topsoils results from the energy balance between convection, conduction, radiation and evapotranspiration (Fig. 6):

$$\phi_{rad} + \phi_{conv} = \phi_{cond} + \phi_{ET} \tag{5}$$

where ϕ_{rad} is the net radiation flux in $W.m^{-2}$ (difference between incident and outgoing radiation fluxes), ϕ_{conv} is the convection flux ($W.m^{-2}$) often approximated by Newton's law of cooling $\phi_{conv} = h(T_{air} - T_{soil})$ with h the convective heat transfer coefficient ($W.m^{-2}.K^{-1}$) and T_{air} and T_{soil} the temperature of air and topsoil respectively, ϕ_{cond} is the conduction flux ($W.m^{-2}$) often approximated by Fourier's law $\phi_{cond} = -\lambda\frac{\partial T}{\partial z}$ with λ the topsoil thermal conductivity ($W.m^{-1}.K^{-1}$), and ϕ_{ET} is the energy flux ($W.m^{-2}$) used in the evaporation of water within topsoils. It is worth noting that this thermal balance on a surface is an approximation since all these physical processes occur over several millimeters or centimeters.

As specified in the introduction, the agriculture community cares about the evapotranspiration to optimize harvesting processes. The Food and Agriculture Organization of the United Nations (FAO) recommends to follow a specific mathematical procedure to compute ϕ_{ET} in Eq. (5). The guidelines [27] propose to compute the evapotranspiration of a reference surface corresponding to "a hypothetical grass reference crop with an assumed crop height of 0.12 m, a fixed surface resistance of 70 $s.m^{-1}$ and an albedo of 0.23". This approximately looks like a classic well-watered grass undergoing weekly precipitations. The evapotranspiration is given by the Penman-Monteith Eq. (6)

$$\phi_{ET} = \frac{\Delta(\phi_{rad} - \phi_{cond}) + \rho_{air} c_p \frac{(e_s - e_a)}{r_a}}{\Delta + \gamma\left(1 + \frac{r_s}{r_a}\right)} \tag{6}$$

where Δ is the slope of the saturation vapor pressure ($kPa.K^{-1}$), ρ_{air} is the air density ($kg.m^{-3}$), c_p is the air specific heat ($J.kg^{-1}.K^{-1}$), $e_s - e_a$ is the air vapor pressure deficit (kPa), r_a is the aerodynamic resistance ($s.m^{-1}$), r_s is the surface resistance ($s.m^{-1}$) and γ is the psychrometric constant ($kPa.K^{-1}$).

In this paper, since we perform calculations over years, we will consider daily-average values in equations. In such a case, the conduction flux in Eq. (6) can be neglected because it is far smaller than the daily-average radiation flux [27]. Besides, the same simplification can be made in Eq. (5) for the same reason.

The guidelines [27] advocate computing the mean saturation vapor pressure $e_s = \frac{e^0(T_{max}) + e^0(T_{min})}{2}$ with

$$e^0(T) = 0.6108 exp\left(\frac{17.27T}{T + 237.3}\right) \tag{7}$$

T_{min} and T_{max} refer to the minimum and maximum daily air temperature (°C). The slope of the saturation vapor pressure temperature is given by

$$\Delta = \frac{4098 e^0(T_{mean})}{(T_{mean} + 237.3)^2} \tag{8}$$

where $T_{mean} = \frac{T_{min} + T_{max}}{2}$ is the mean temperature relatively to the minimum and the maximum daily temperatures. The actual vapor pressure is calculated from the relative humidity RH

$$e_a = \frac{e^0(T_{min})RH_{max}/100 + e^0(T_{max})RH_{min}/100}{2} \tag{9}$$

The psychrometric constant is calculated with $\gamma = 6.65 \times 10^{-4} PkPa.^\circ C^{-1}$ with P the atmospheric pressure. If the measurements of wind speed and relative humidity are achieved at approximately 1 meter above ground, $r_a \sim \frac{158}{V_{wind}}$ with V_{wind} the wind speed. The general equation for r_a is provided in [27]. Eventually, the FAO suggests $r_s \sim 70 s.m^{-1}$.

With this empirical procedure, we can calculate ϕ_{ET} in Eq. (5) from our radiation measurements. It is worth noting that Eq. (6) gives the evapotranspiration flux for the reference surface detailed above. We assume the value of ϕ_{ET} for Lascaux to be close to the value given for the reference surface.

In Eq. (5), it only remains the convective heat transfer coefficient to estimate. The studies [28] about this issue often use an empirical relation. Here, we propose another calculation which ensures the conservation of energy with a time average convective heat transfer coefficient. This calculation only requires to measure the temperature just below the ground surface. The time average of Eq. (5) yields

$$\overline{\phi_{rad}} + h\left(\overline{T_{air}} - \overline{T_{soil}}\right) \sim \overline{\phi_{ET}} \tag{10}$$

The energy conservation implies $\overline{T_{soil}} \sim \overline{T_{mes,depth}}$ where $\overline{T_{mes,depth}}$ is the average temperature measured underground. The approximate equality between both average temperatures is particularly true when the measurement in depth is close to the ground surface since the phase change remains small. The period in the time average must thus be chosen to be far greater than the phase change between the surface temperature and the measurement in depth. Here, the closest thermocouple is 50 cm in depth (§2), which leads to a phase change of approximately 2 weeks for annual thermal waves. We have thus chosen an annual average in Eq. (10). This allows us to calculate the convective heat transfer coefficient with

$$h = \frac{\left(\overline{\phi_{ET}} - \overline{\phi_{rad}}\right)}{\left(\overline{T_{air}} - \overline{T_{mes,depth}}\right)} \tag{11}$$

It is worth noting that measuring the temperature just below the ground surface would allow the calculation of weekly average coefficients for instance, which would significantly improve the accuracy of the results.

The thermal boundary condition in the numerical simulations presented in Sections 4 & 5 is thus

$$T_{soil} \sim T_{air} + \frac{\phi_{rad} - \phi_{ET}}{h} \tag{12}$$

4. Application to the Lascaux Cave

4.1. Rock thermal diffusivity

For each cave thermocouple, we assess the thermal diffusivity based on the phase changes (Eq. (3)) and the thermal damping (Eq. (4)). Fig. 7 displays the graphical estimations of both parameters for each thermocouple except those 50 and 100 cm in depth. The uncertainty is indeed greater near the surface since the topsoil thickness is less negligible for shallow thermocouples than for cave thermocouples. These measurements have thus been excluded. Based on phase change, the optimized thermal diffusivity calculated with a least squares regression is approximately $1.7 \times 10^{-6} m^2.s^{-1}$. Based on thermal damping, the approximated least-squares thermal diffusivity is $1.3 \times 10^{-6} m^2.s^{-1}$. Both values are typical diffusivities for limestone.

The standard deviation associated with phase change is $7.5 \times 10^{-7} m^2.s^{-1}$, which is almost equal to half the least squares solution. For damping, the standard deviation is $1.5 \times 10^{-6} m^2.s^{-1}$ which is greater than the global thermal diffusivity. There is thus a great disparity between the results, suggesting that the rock mass is not thermally homogeneous. Based on both calculated diffusivities, Fig. 8 gives the range of the mean rock diffusivity above each thermocouple, under the assumption of 1D heat propagation. This reveals that for most thermocouples, there is an inconsistency between damping and phase change. The average gap between both diffusivities is approximately $7.6 \times 10^{-7} m^2.s^{-1}$, which corresponds to half the average diffusivity, leading to significant deviations. The reason of this decoupling can be the heterogeneity of limestone in the surrounding of the Lascaux Cave [21,22]. In Section 4.3, we will compare the measurements of two thermocouples (C6 and E1) within the cave with the results providing by the 1D homogeneous model.

4.2. Shallow temperature

We compare here the calculated (Eq. (1)) and measured temperatures 50 and 100 cm below the surface, at locations O (beneath oaks), P (beneath pines) and S (in full sun) (Fig. 3). The annual average net radiation is approximately $30 W.m^{-2}$, $15 W.m^{-2}$ and $80 W.m^{-2}$ beneath oaks, pines and in direct sunlight respectively. The analysis will be based on two error measures. The mean absolute error is given by

$$\frac{1}{N} \sum_{i=1}^{N} |T_{cal,i} - T_{mes,i}| \tag{13}$$

It provides the average gap between the calculated and measured temperatures. The efficiency is given by

$$1 - \frac{\sum_{i=1}^{N} \left(T_{cal,i} - T_{mes,i}\right)^2}{\sum_{i=1}^{N} \left(T_{mes,i} - \overline{T_{mes}}\right)^2} \tag{14}$$

It compares the residual variance to the variance of the measured data. This yields the part explained by the model. Fig. 9 compares the simulated temperature with the measurements at the six points (O1, O2, S1, S2, P1, P2) over five years. Table 1 details the error coefficients for the six measurements. To obtain these results, the thermal diffusivity has been adjusted. The diffusivity is $4 \times 10^{-7} m^2.s^{-1}$ for O1 and O2, $2 \times 10^{-7} m^2.s^{-1}$ for P1 and P2, and $5 \times 10^{-7} m^2.s^{-1}$ for S1 and S2. These values are different from the rock thermal diffusivities calculated in §4.1. The geological nature under the Lascaux pines corresponds to detrital formations (Fig. 2) [22] which present low thermal diffusivities. At locations O and S, there are first a thin layer composed of common constituents of topsoils, and then limestone. The diffusivity of limestone is of the order of $10^{-6} m^2.s^{-1}$ [29], so greater than the adjusted thermal diffusivities. Water could explain these low thermal diffusivities, since porous limestone contains water, especially near the surface. Such a behavior has indeed been observed at Lascaux based on electrical resistivity tomography [30]. The estimation of the equivalent thermal diffusion coefficient can be estimated by Eq. (15):

$$D_{eq} = \frac{(1-\epsilon)\lambda_{rock} + \epsilon\left(\chi\lambda_{water} + (1-\chi)\lambda_{air}\right)}{(1-\epsilon)\rho_{rock}C_{p,rock} + \epsilon\left(\chi\rho_{water}C_{p,water} + (1-\chi)\rho_{air}C_{p,air}\right)} \tag{15}$$

with λ the thermal conductivity, C_p the specific heat, ρ the density, ϵ the porosity of rock and χ the water saturation. With a fracture porosity of 0.3 [25] (§3.1), a water saturation of 0.9, a limestone conductivity of $2 W.m^{-1}.K^{-1}$, a specific heat of $700 J.kg^{-1}.K^{-1}$ and a density of $2500 kg.m^{-3}$ (typical properties for limestone), the equivalent thermal diffusivity is $6 \times 10^{-7} m^2.s^{-1}$. The order of magnitude

Table 1
Mean absolute error and efficiency calculated at points O1, O2, P1, P2, S1 and S2.

	O1	O2	P1	P2	S1	S2
Mean absolute error (°C)	0.65	0.4	0.48	0.25	0.46	0.33
Efficiency	0.96	0.98	0.97	0.98	0.96	0.98

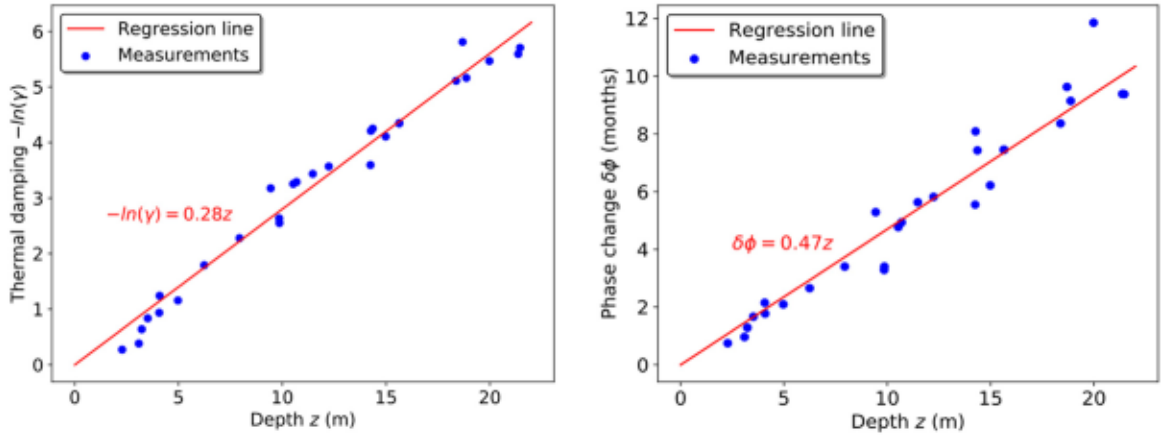

Fig. 7. Thermal damping and phase change according to depth for all the thermocouples strictly deeper than 1 meter.

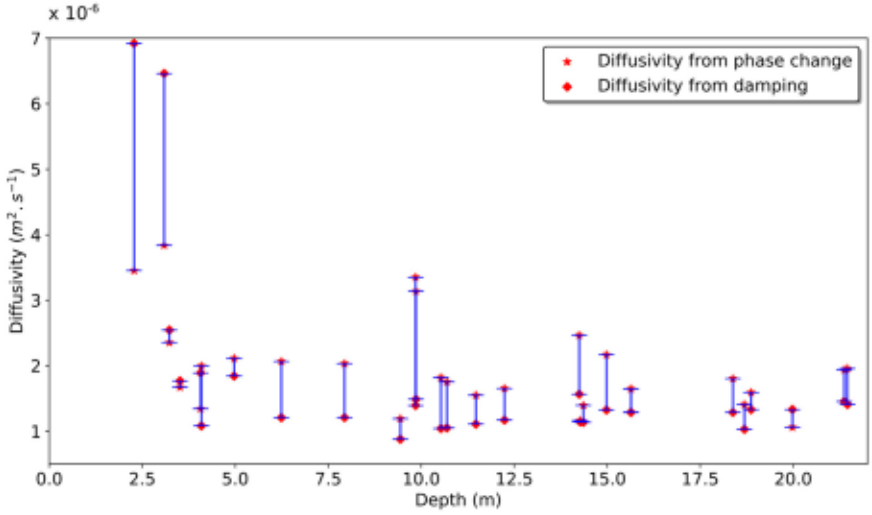

Fig. 8. Thermal diffusivity range for each thermocouple deeper than 1 meter.

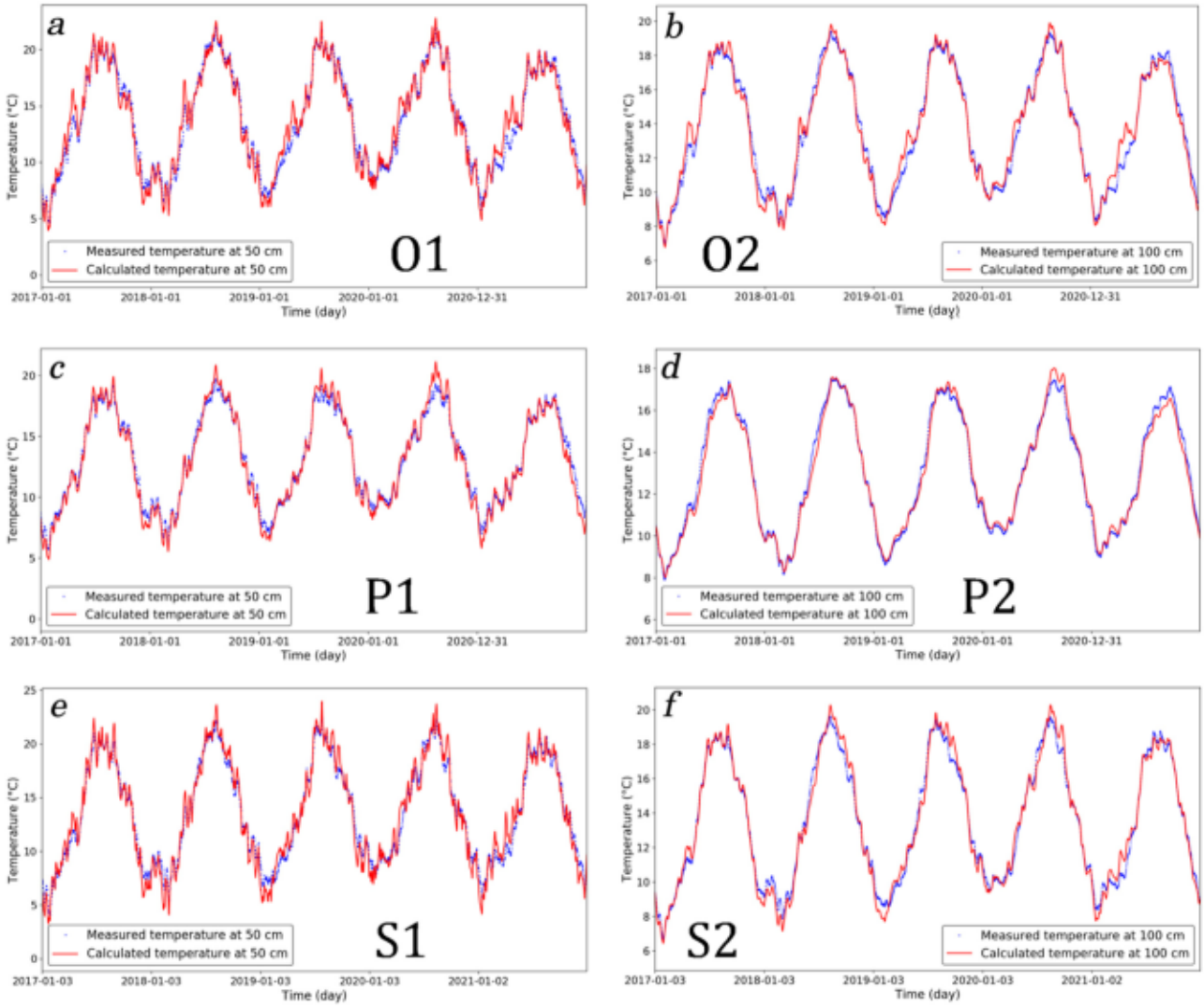

Fig. 9. Measured and calculated temperatures at a) O1, b) O2, c) P1, d) P2, e) S1 and f) S2 (Fig. 2).

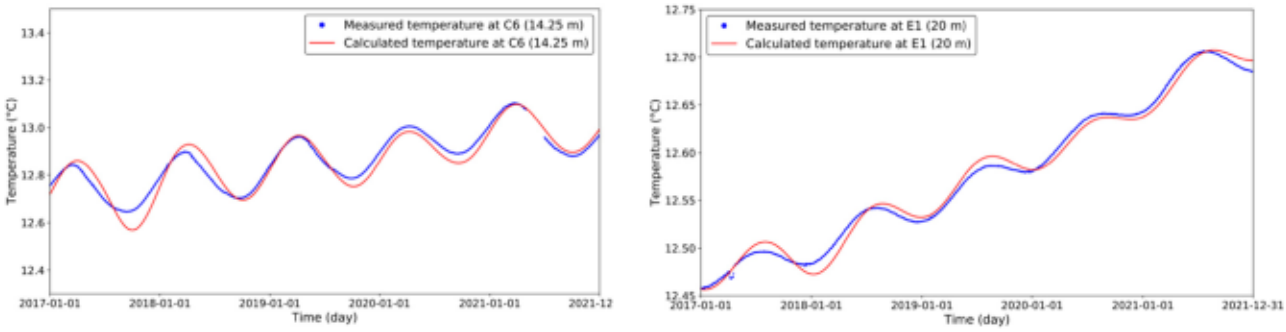

Fig. 10. Calculated and measured temperature at C6 and E1.

of the diffusion coefficients can thus be explained by the complex composition of the top part of the rock mass.

The model successfully calculates temperatures close to the measurements. The efficiency at the six locations is indeed very close to 1, which indicates small errors in the predictions. The average gap between simulation and experiment is always of a few tenth of degrees according to the mean absolute errors. This deviation must be compared with the actual temperature presenting annual variations of approximately 15 °C at 50 cm, and 10 °C at 100 cm. The maximal mean error thus appears for O1 with only 5% of the wave amplitude.

This difference could result from the calculation procedure of the surface temperature. For instance, the calculated ETP corresponds to a reference configuration (grass) whereas the Lascaux hill is mainly covered by trees. In addition, the convective heat transfer coefficient is assumed to be constant over a year, which inevitably leads to discrepancies. The variation of the water saturation must impact the thermal diffusivity, which thus must be time dependent. This could also affect the accuracy of the model. However, despite these error sources, the gap between the measurements and the calculations is low. The 1D homogeneous thermal conduction model with an energy balance at the ground surface thus provides very satisfactory results in the first meter.

4.3. Temperature in the cave

We compare the calculated temperatures with the measurements at two locations. We choose the two thermocouples among those presenting a weak difference between both estimated diffusivities (Fig. 8). We will discuss about this choice in Section 5. We select thermocouples C6 (14.25 m) and E1 (20 m) (Fig. 2) and compare temperatures over 5 years in Fig. 10. Because the thermal conduction in rock is a slow process, we make the simulations start in 2014 while only the results from 2017 are considered in the paper. These calculations need to be initialized with a temperature field. We use the analytical solution (Eq. (2)) where the maximal and minimal temperatures are adjusted to the measured temperatures during 2013 in order to apply a temperature field close to reality. To compute the ground surface temperature, we choose the configuration P as it is the most consistent with the measurements. There is indeed no outside experimental apparatus right above C6 and E1.

According to Fig. 8, both estimated diffusivities are very similar at C6, so the good agreement with the model was expected with a diffusivity of $1.2 \times 10^{-6} m^2.s^{-1}$. The mean error is approximately 0.03 °C over five years, which corresponds approximately to 15% of the wave amplitude at this depth. This error mainly concerns the first two years, where the amplitude and the time delay of the calculated wave are greater than those of the measured wave. This deviation could stem from a variation of the thermal diffusivity according to time, due to water saturation for instance. There is also an uncertainty on the ground surface temperature since there is no experimental setup outside, right above thermocouple C6. The amplitude of the measured thermal wave indeed seems to vary weakly over five years, contrary to the calculated temperature where the amplitude is greater for the first two years. This difference could thus be related to the top boundary temperature. The same discussion holds for thermocouple E1. With a diffusivity of $1.1 \times 10^{-6} m^2.s^{-1}$, the mean error is 0.006, so approximately 20% of the wave amplitude 20 m underground. Like C6, the gap is greater during the first two years. The error source therefore seems to be the same as for C6.

For both locations, the model presents higher deviations than close to the ground surface of the cave rock mass. This was expected since the deeper, the more the heat propagation is three-dimensional. Despite this, the 1D model calculates temperatures in the expected range, with a rather low error considering the simplicity of the hypotheses.

5. Discussion

5.1. Ground surface temperature

The calculation of the ground surface temperature (§3.2.2) requires the study site to be heavily instrumented with radiation and relative humidity sensors, anemometers and thermocouples. To study the thermal behavior of the cave, such a device must be installed at as many points as possible. Knowing the surface temperature right above the cave is obviously of great importance, but due to 3D effects, the temperature is also necessary in its vicinity. Ideally, a network of soil sensors covering an area encompassing the cave should be set up. This would allow accurate interpolations everywhere above the cave.

However, this choice would necessitate a very heavy and costly instrumentation. This could be avoided by introducing thermocouples into the first few centimeters of topsoil. They would directly measure temperatures in topsoil resulting from the complex energy balance at the ground surface (§3.2.2). This temperature could then be considered as the boundary condition in the numerical resolution of the heat Eq. (1). This methodology prevents uncertainties on the radiation and the wind speed measurements, but also the approximations in the theoretical calculation of the surface temperature.

As regards the temperature calculation within the first meter of the rock mass, the 1D homogeneous model provides very satisfying results. The error remains negligible despite complex and time-dependent phenomena which are difficult to assess accurately. It is worth noting that a good understanding of water saturation according to time could further enhance the precision of the model. This might be done for the Lascaux Cave since rainfall and the electrical resistivity of the rock mass are continuously measured. This would also require an advanced modeling of the water bal-

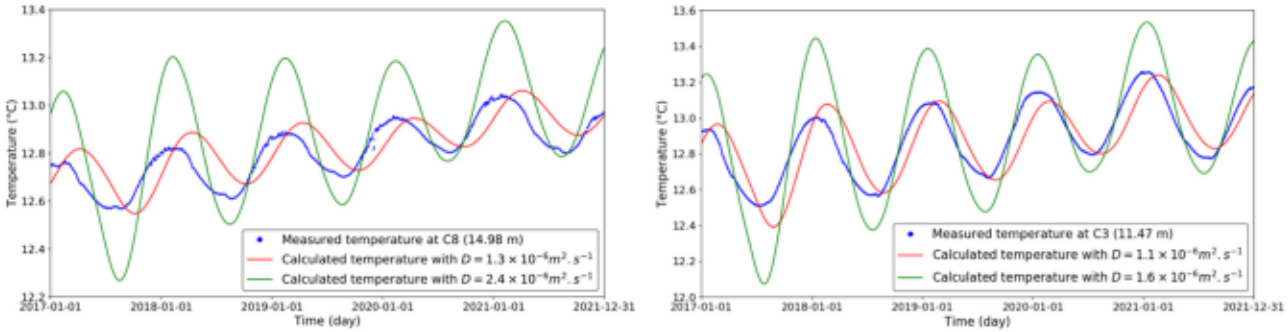

Fig. 11. Measured and calculated temperatures corresponding to thermocouples C8 and C3 (Fig. 3). For each thermocouple, both calculated temperatures are based on two different thermal diffusivities respectively leading to a phase change and a damping consistent with the measurements.

ance within the rock mass. The weak depth of the measurements seems to make the 1D homogeneous hypothesis reliable. With a thorough instrumentation of the site surface as described above, the thermal behavior of the upper part of the rock mass would therefore be known with great accuracy.

5.2. Cave temperature

The temperature within the cave has been compared for two thermocouples (C6 and E1) in Section 4.3. Both locations have been chosen among the most prone to be thermally predictable by a 1D homogeneous model. The measurements at these points indeed show a good correlation between the phase change and the thermal damping (Fig. 8), which can be explained with a uniform thermal diffusivity. For these thermocouples, the calculated temperatures are close to the measurements, with a mean absolute error (Eq. (13)) smaller than 20% of the wave amplitude over 5 years and an efficiency (Eq. (14)) greater than 0.95. For most applications (waste storage, geothermics, temperature correction for electrical resistivity measurements, etc.), this model is thus very satisfactory and provides results accurate enough. However, in the particular case of thermo-aeraulic simulations in caves, a precision of a few hundredths of degrees is necessary. In details, for other thermocouples such as C8 or C3 for instance (Fig. 3), one cannot accommodate the phase change and the damping under the homogeneous assumption. Fig. 11 compares the measured temperature with two calculated temperatures where the thermal diffusivity is equal to either $1.3 \times 10^{-6}\ m^2.s^{-1}$ or $2.4 \times 10^{-6}\ m^2.s^{-1}$ for C8, and $1.1 \times 10^{-6}\ m^2.s^{-1}$ or $1.6 \times 10^{-6}\ m^2.s^{-1}$ for C3. For each location, both diffusivities have been chosen to make the calculated temperature fit with the wave damping and the phase change respectively.

Figure 11 shows that for C8 and C3, there is no thermal diffusivity being able to reproduce aptly the measured temperatures. Satisfying the phase change and the wave damping requires a more complex model with a non-constant diffusivity. The domain could be divided into two parts with two distinct thermal diffusivities. From a mathematical point of view, these two unknowns could be adjusted to fit with both the phase change and the thermal damping. However, this can be done at one location but there is no reason that the two calculated diffusivities could yield satisfactory results at other locations in such a complex karstic system. The homogeneous hypothesis fails to explain the measurements at C8 and C3, contrary to C6 and E1 (§4.3). The study about the phase change and the thermal damping in Section 4.1, which is based on a simple analytical solution, can therefore allow scientists to predict whether the thermal study of a rock mass can rely on the homogeneous assumption. In the case of the Lascaux Cave, the rock mass should be considered as heterogeneous. To improve the results presented in the prior section, a more complex 3D heterogeneous model must be considered. Water circulation in rock must also impact the thermal diffusivities according to time. Therefore, using constant heterogeneous properties might also be insufficient to get accurate results. A coupling between a 3D heterogeneous model and a water circulation model could thus be required.

As stated in the introduction, the thermal behavior of caves is always investigated with homogeneous models. Scientists must ensure that the studied rock mass is really homogeneous, which never happens for karstified rock masses such as those surrounding caves. This is a paramount issue since high precision is necessary when studying caves thermally. Indeed, the onset of the thermal convection is very sensitive to thermal gradients and a few hundredth of degrees can distort predictions.

6. Conclusion

For the sake of cave conservation, the investigation of the heat propagation in rock masses is an important matter. The temperature of the cave walls indeed drives the thermal convection within cavities, which causes potential alterations. At present, the studies in the domain are based on the resolution of the 1D heat equation with a constant thermal diffusivity. The ground surface temperature is also supposed to be equal to the outside air temperature.

However, we have shown that the ground surface temperature is different from the outside air temperature. Our temperature measurement a few centimeters into the ground has revealed a significant loss of energy, indicating that a complex physical process should take place at the surface. Based on literature, especially in agriculture, we have detailed such phenomena. The ground surface temperature actually results from an energy balance involving radiation, convection, conduction and water evaporation. The surface temperature thus requires many measurements and empirical calculations. To ensure the energy conservation in the standard mathematical procedure, we have proposed a suitable formula for the convective heat transfer coefficient.

This strategy has then been applied to the Lascaux Cave which has been heavily instrumented for decades. The calculated temperatures the first meter below the ground surface have been satisfactorily compared with measurements, whatever the radiation configuration. The low error indicates that the proposed model, relying on the 1D homogeneous hypothesis, is sufficient to simulate the thermal behavior close to the surface. Inside the cave, the model successfully computes the temperature at carefully chosen locations, where we expected the homogeneous assumption to be reliable. Elsewhere, the phase change and the thermal damping cannot be explained by such a simple model. The homogeneous hypothesis is very likely inconsistent with the geology of the rock mass. The assessment of the thermal diffusivities matching the measured phase change and damping for each thermocouple has highlighted the limitations of this assumption. For heteroge-

neous rock masses, such as in Lascaux, the current model cannot aptly describe the heat propagation over 10 m. Instead, a 3D heterogeneous model should be considered for thermal simulations.

In order to simulate the thermal convection in the Lascaux Cave, we need a model to evaluate the wall temperature. Based on electrical resistivity tomography measurements, a geophysics investigation is currently conducted on the Lascaux rock mass. Its geological heterogeneities are being characterized and localized spatially. This will allow us to subdivide the Lascaux rock mass into a few homogeneous subareas. Then, a study will address the thermal characterization of the cave rock mass to be able to simulate the heat propagation with heterogeneous properties. More broadly, the strategy developed in the paper should be applied to other caves concerned by conservation issues. Underground cavities like mines or waste storage capacities could also necessitate such a thermal investigation.

Declaration of Competing Interest

The authors declare that they have no known competing financial interests or personal relationships that could have appeared to influence the work reported in this paper.

CRediT authorship contribution statement

F. Salmon: Conceptualization, Writing – original draft. **D. Lacanette:** Conceptualization, Writing – review & editing, Supervision. **H. Lharti:** Conceptualization, Writing – review & editing. **C. Sirieix:** Conceptualization, Writing – review & editing, Supervision.

Data availability

The authors do not have permission to share data.

Acknowledgements

We thank the Ministry of Culture and the DRAC Nouvelle-Aquitaine for providing funding for the project and for their investment in the experimental instrumentation of the Lascaux site. We also thank Muriel Mauriac, curator of the cave. We are grateful to Jean-Christophe Portais for providing experimental data and achieving measurements when necessary.

References

[1] M. Lönnqvist, H. Hökmark, Thermal, mechanical and thermo-mechanical assessment of the rock mass surrounding SKB's prototype repository at Äspö HRL, Rock Mech. Rock Eng. 49 (2016) 1123–1142.
[2] N. Sultan, P. Delage, Y.J. Cui, Comportement thermomécanique de l'argile de Boom, Comptes Rendus de l'Académie des Sciences - Series IIB – Mech. 328 (6) (2000) 457–463.
[3] P. Berest, Heat transfer in salt caverns, Int. J. Rock Mech. Min. Sci. 120 (2019) 82–95.
[4] B. Sanner, C. Karytsas, D. Mendrinos, L. Rybach, Current status of ground source heat pumps and underground thermal energy storage in Europe, Geothermics 32 (4–6) (2003) 579–588.
[5] H. Yang, P. Cui, Z. Fang, Vertical-borehole ground-coupled heat pumps: a review of models and systems, Appl. Energy 87 (1) (2010) 16–27.
[6] P. Bérest, F. Louvet, Aspects of the thermodynamic behavior of salt caverns used for gas storage, Oil Gas Sci. Technol. – Rev. *IFP Energies nouvelles* 75 (2020) 57.
[7] D. Lacanette, S. Vincent, A. Sarthou, P. Malaurent, J.-P. Caltagirone, An Eulerian/Lagrangian method for the numerical simulation of incompressible convection flows interacting with complex obstacles: application to the natural convection in the Lascaux cave, Int. J. Heat Mass Transf. 52 (2009) 2528–2542.
[8] D. Domínguez-Villar, I.J. Fairchild, A. Baker, R.M. Carrasco, J. Pedraza, Reconstruction of cave air temperature based on surface atmosphere temperature and vegetation changes: implications for speleothem palaeoclimate records, Earth Planet. Sci. Lett. 369 (370) (2013) 158–168.
[9] D. Domínguez-Villar, K. Krklec, J.A. López-Sáez, F.J. Sierro, Thermal impact of Heinrich stadials in cave temperature and speleothem oxygen isotope records, Quat. Res. 101 (2021) 37–50.
[10] B. Guerrier, F. Doumenc, A. Roux, S. Mergui, P.-Y. Jeannin, Climatology in shallow caves with negligible ventilation: heat and mass transfer, Int. J. Therm. Sci. 146 (2019) 106066.
[11] David Domıńguez-Villar, S. Lojen, K. Krklec, A. Baker, I.J. Fairchild, Is global warming affecting cave temperatures? Experimental and model data from a paradigmatic case study, Clim. Dyn. 45 (3) (2015) 569–581.
[12] F. Perrier, P. Morat, T. Yoshino, O. Sano, H. Utada, O. Gensane, J.-L.Le Mouël, Seasonal thermal signatures of heat transfer by water exchange in an underground vault, Geophys. J. Int. 158 (2004) 372–384.
[13] M. Luetscher, P.Y. Jeannin, Temperature distribution in karst systems: the role of air and water fluxes, Terra Nova 16 (2004) 344–350.
[14] A. Bögli, Karst Hydrology and Physical Speleology, Springer, Berlin, 1980.
[15] M.S. Roxy, V.B. Sumithranand, G. Renuka, Soil heat flux and day time surface energy balance closure at astronomical observatory, Thiruvananthapuram, south Kerala, J. Earth Syst. Sci. 123 (4) (2014) 741–750.
[16] B. Larwa, Heat transfer model to predict temperature distribution in the ground, Energies 12 (1) (2019) 25.
[17] R. Li, X. Hou, Z. Jia, Q. Han, X. Ren, B. Yang, in: Effects on Soil temperature, moisture, and Maize Yield of Cultivation with Ridge and Furrow Mulching in the Rainfed Area of the Loess Plateau, 116, Agricultural Water Management, China, 2013, pp. 101–109.
[18] P. Hlavinka, M. Trnka, J. Balek, D. Semerádová, M. Hayes, M. Svoboda, J. Eitzinger, M. Možný, M. Fischer, E. Hunt, Z. Žalud, Development and evaluation of the SoilClim model for water balance and soil climate estimates, Agric. Water Manag. 98 (8) (2011) 1249–1261.
[19] R.J. Lascano, R.L. Baumhardt, Effects of crop residue on soil and plant water evaporation in a dryland cotton system, Theor. Appl. Climatol. 54 (1996) 69–84.
[20] N. Aujoulat, J.-J. Cleyet-Merle, J. Gaussen, N. Tisnerat, H. Valladas, Approche chronologique de quelques sites ornés paléolithiques du Périgord par datation Carbone 14 en spectrométrie de masse par accélérateur de leur mobilier archéologique, Paléo (1998) 319–323.
[21] C. Verdet, C. Sirieix, A. Marache, J. Riss, J.-C. Portais, Detection of undercover karst features by geophysics (ERT) *Lascaux* cave hill, Geomorphology 360 (2020) 107177.
[22] S. Xu, C. Sirieix, A. Marache, J. Riss, P. Malaurent, 3D geostatistical modeling of Lascaux hill from ERT data, Eng. Geol. 213 (2016) 169–178.
[23] H. Lharti, C. Sirieix, J. Riss, C. Verdet, D. Lacanette, Clustering methods applied to electrical resistivity data, in: NSG2022 28th European Meeting of Environmental and Engineering Geophysics, 2022, 2022, pp. 1–5.
[24] C. Verdet, PhD Thesis, 2019.
[25] S. Xu, Caractérisation de l'environnement karstique de la grotte de Lascaux par couplage de méthodes géophysique, statistique et géostatistique, PhD Thesis, 2015.
[26] D.A. De Vries, Thermal properties of soils, in: W.R. van Wijk (Ed.), Physics of Plant Environment, North-Holland Publishing Company, Amsterdam, 1963.
[27] R.G. Allen, L.S. Pereira, D. Raes, M. Smith, Crop Evapotranspiration —Guidelines for Computing Crop Water requirements. FAO Irrigation and Drainage Paper 56, Food and Agriculture Organization, Rome, 1998.
[28] M. Chalhoub, M. Bernier, Y. Coquet, M. Philippe, A simple heat and moisture transfer model to predict ground temperature for shallow ground heat exchangers, Renew. Energy 103 (2017) 295–307.
[29] E.C. Robertson, Open file report, 1988, pp. 88–441.
[30] C. Verdet, C. Sirieix, J. Riss, D. Lacanette, An ERT time-lapse method to characterize water movements in a karstic medium, 26th European Meeting of Environmental and Engineering Geophysics, 2020.